Carbohydrate Polymers 81 (2010) 524–532

Contents lists available at ScienceDirect

Carbohydrate Polymers

journal homepage: www.elsevier.com/locate/carbpol

Structural differences between hot-water-soluble and hot-water-insoluble fractions of starch in waxy rice (*Oryza sativa* L.)

Rosa Paula Cuevas[a,b], Robert G. Gilbert[b], Melissa A. Fitzgerald[a,*]

[a] *Grain Quality, Nutrition and Postharvest Center, International Rice Research Institute (IRRI), DAPO 7777 Metro Manila, Philippines*
[b] *The University of Queensland, Centre for Nutrition and Food Sciences, LCAFS, Brisbane, Qld 4072, Australia*

ARTICLE INFO

Article history:
Received 14 December 2009
Received in revised form 27 February 2010
Accepted 2 March 2010
Available online 9 March 2010

Keywords:
Hot-water-soluble starch
Structural properties
Chain-length distributions
Degree of branching

ABSTRACT

Amylose readily dissolves in hot water, unlike amylopectin which is largely insoluble. However, size distributions of amylose isolated in such a manner often show the presence of hyper-branched material consistent with amylopectin. The difference in solubility suggests that the hot-water-soluble (HWS) hyper-branched material might be structurally distinct from typical amylopectin. In the present paper, the structural properties of the two solubility fractions of hyper-branched material are explored in a set of traditional waxy rice varieties. The objective was to elucidate the nature of the HWS component, e.g. to see if it could be phytoglycogen, another water-soluble polysaccharide. We show that solubility is controlled by thermodynamic effects, rather than slow dissolution (kinetic effects). The average size, degree of branching and the debranched chain-length distributions indicate that the HWS fraction is structurally different from phytoglycogen. The debranched chain-length distributions of short chains and the degrees of branching in the HWS material are similar to those of the hot-water-insoluble (HWI) fractions but the chain-length distributions indicate that the HWI fractions carry longer chains than those in the HWS fractions. Light-scattering measurements show that the average size of whole molecules in the HWI component is significantly greater than in the HWS component. It is postulated that the structural differences limit solubility of the molecules in the HWI fraction, possibly due to co-crystallisation with adjacent molecules at more points than is possible for the shorter chains in HWS molecules.

1. Introduction

It is common practice to separate starch from flour into two components: those that are readily hot-water soluble (HWS) and those that remain hot-water insoluble (HWI). In non-waxy varieties, it commonly assumed that amylose can be separated from amylopectin by aqueous dispersion in hot water (Chinnaswamy & Bhattacharya, 1986; Cowie & Greenwood, 1957; Kim & Willett, 2004; Roger & Colonna, 1996; Ward, Gao, de Bruyn, Gilbert, & Fitzgerald, 2006). The question arises as to the completeness of such a separation, and the structural reason for obtaining a HWI and HWS fraction. In hot water, crystalline regions in the amylopectin molecules melt, or gelatinise (Slade & Levine, 1988). Once these regions have melted, the granules swell, and those components that are soluble leach out of the granules into the surrounding water. The amounts and the structures of these components are thought to influence textural properties of starch (Fitzgerald, 2004).

Size exclusion chromatography (SEC) shows that the water-soluble fraction of non-waxy starch generally exhibits a peak associated with amylopectin as well as the expected amylose peak (Mizukami, Takeda, & Hizukuri, 1999; Ong & Blanshard, 1995; Ramesh, Ali, & Bhattacharya, 1999; Ward et al., 2006).

The properties of the water-soluble glucan are consistent with it being highly branched (Juliano, Perez, Kaushik, & Khush, 1990): it stains red upon reaction with iodine and its lambda maximum value is about 530–570 nm (Bultosa, Hamaker, & BeMiller, 2008; Miklus & Hamaker, 2003; Mizukami et al., 1999; Ramesh et al., 1999). The size distribution of the chains detected by SEC after debranching is similar to that of native amylopectin (Miklus & Hamaker, 2003; Mizukami et al., 1999). While these data suggest that the molecules are hyper-branched glucans, it is not sufficient evidence to conclude that the molecules are structurally similar to amylopectin. SEC is less sensitive to changes in short chains (Castro, Ward, Gilbert, & Fitzgerald, 2005) and is prone to band broadening (Castro, Ward, et al., 2005; Konkolewicz, Taylor, Castignolles, Gray-Weale, & Gilbert, 2007; van Berkel, Russell, & Gilbert, 2005).

Phytoglycogen is a water-soluble polysaccharide. Like amylopectin, phytoglycogen is composed of glucose units joined linearly by α-1,4 glycosidic linkages with branches linked at α-1,6 positions (Fujita et al., 2003). Chain-length distributions have been used to distinguish phytoglycogen from amylopectin (Burton et al., 2002; Kubo et al., 1999; Nakamura, 2002; Wong et al., 2003) in isoamylase-deficient mutants. In these mutants, there are higher proportions of A ($X \leq 12$) and B2 ($25 \leq X \leq 36$) chains (Burton et al.,

* Corresponding author. Tel.: +632 580 5600; fax: +632 580 5699.
E-mail address: m.fitzgerald@cgiar.org (M.A. Fitzgerald).

0144-8617/$ – see front matter © 2010 Elsevier Ltd. All rights reserved.
doi:10.1016/j.carbpol.2010.03.007

2002; Kubo et al., 1999; Manners, 1989) in the water-soluble fraction than in the insoluble fraction. These additional branches confer a spherical shape to molecules of phytoglycogen, and limit the size the molecules reach (Manners, 1991).

The molecules in the HWS fraction could have structure comparable to that of phytoglycogen. However, in contrast to the HWS fraction, phytoglycogen is normally extracted in chilled conditions (Burton et al., 2002; Delatte, Trevisan, Parker, & Zeeman, 2005; Dinges, Colleoni, Myers, & James, 2001). The use of hot water to extract the components of the HWS fraction implies that it forms part of the starch granule. It is either the product of reduced debranching enzyme activity, which causes slower crystallisation (hence its solubility), or it is pre-amylopectin which is partly incorporated into the starch granule—the crystalline portion is within the granule while the soluble portion could be exposed to further starch synthase and branching enzyme activity, leading to phytoglycogen synthesis (Myers, Morell, James, & Ball, 2000). The structure of the HWS component, whether consistent with that of amylopectin or of phytoglycogen, should be established.

The presence of this HWS fraction is a feature of the starch which potentially relates to sensory properties. In this study, we use a diagnostic tool (Cuevas et al., 2010) to investigate the HWS and the HWI fractions. The plots of the log of the number distribution of the debranched glucan (Castro, Dumas, Chiou, Fitzgerald, & Gilbert, 2005) will be used to search for differences between phytoglycogen, branched glucans in the HWS and the HWI fractions. The hyper-branched glucans in the water-soluble fraction require analysis on as many structural levels as possible to determine whether the soluble and insoluble molecules differ only in size distribution, or also in degree of branching or in the arrangement of the chains within the molecules. Such an investigation is simplified if the material does not contain amylose. Using a set of traditional waxy rice varieties from the Lao PDR, the objectives of this study are: (a) to confirm whether the HWS hyper-branched glucans differ structurally from the HWI fraction of the starch in waxy varieties of rice and (b) to determine whether the insolubility of the HWI fraction is thermodynamic or kinetic, i.e., whether the fraction is truly insoluble in hot water, or alternatively, if it would eventually all dissolve if the system were truly equilibrated.

2. Materials and methods

2.1. Materials

Paddy rice grains of fifty-six traditional Lao waxy rice varieties were obtained from the TT Chang Genetic Resources Center of the International Rice Research Institute (IRRI). These were grown and harvested in IRRI fields in the dry seasons of 2000–2002 and 2004–2005, or in the wet season of 2006. The paddy grains were dehulled (Satake Rice Machine, Tokyo, Japan) and milled (Grainman 60-230-60-2AT, Grain Machinery Mfg. Corp., Miami, FL, USA). Milled grains of Med Gnay, Laboun, Hom, Makfay, Phae Noy, and Phae Savan were obtained from the International Network for Genetic Evaluation of Rice (INGER) at IRRI. Variety names and identifiers are presented in Supplementary material. Milled grains were ground (Udy Cyclone Sample Mill 3010-030, Fort Collins, CO, USA) to pass through a 0.5 mm sieve. Reagent-grade chemicals and reverse-osmosis water (filtered through a 0.22 μm Millipore filter) were used throughout the study.

2.2. Gelatinisation temperature of waxy rice varieties

Gelatinisation temperature was measured using differential scanning calorimetry following a published method (Cuevas et al., 2010).

2.3. Quantification of HWS and HWI fractions

Flour (25 mg) of each sample was suspended in 1.25 mL water and heated at 95 °C for 10 min with constant stirring. The suspension was then centrifuged (10 min, 14,000 × *g*). The pellet (containing the HWI fraction) and the supernatant (containing the HWS fraction) were dried in a centrifugal vacuum dryer (SpeedVac, Sunnyvale, CA, USA). The dried fractions were subsequently weighed.

2.4. Separation of HWS and HWI fractions

The methodology for separation and debranching of the HWS and the HWI fractions from flour is given elsewhere (Ward et al., 2006). In brief, flour was suspended in hot water, centrifuged and each fraction was enzymatically debranched using isoamylase (Megazyme, Wicklow, Ireland). Samples were prepared in duplicate.

2.5. Debranched chain-length distributions

The chain-length distribution of debranched material from the two fractions was determined by SEC and by fluorophore-assisted capillary electrophoresis (FACE).

2.5.1. FACE

An aliquot (100 μL) of each fraction was dried using the centrifugal vacuum dryer. Maltose, a mobility marker, was added to the dried sample and the mixture was dried in the centrifugal vacuum dryer. Conditions during the labelling reaction and during separation were as previously described (O'Shea, Samuel, Konik, & Morell, 1998) except that labelling was done at 50 °C for 16 h, and FACE was conducted for 60 min. The P/ACE MDQ capillary electrophoresis system (Beckman-Coulter, Fullerton, CA, USA) was equipped with a laser-induced fluorescence detector and an argon lamp (light source). Separation was conducted on a carbohydrate-coated capillary (I.D. = 50 μm, Beckman-Coulter), which was controlled and recorded by the 32-Karat® (Version 7.0) software. Chain lengths (degrees of polymerisation) were assigned per peak based on the migration of maltose. Peak area was converted to velocity-area (Demorest & Dubrow, 1991) to obtain the relative number of chains, $N(X)$, with degree of polymerisation (DP) X.

2.5.2. SEC

The remaining debranched material was desalted with mixed bed resin (AG 501-X8, Bio-Rad, Hercules, CA, USA) for 45 min. The samples were held at 40 °C by a heater in the autosampler. Aliquots (40 μL) were injected, and separation was conducted for 36 min on a Waters (Milford, MA, USA) HPLC system comprised of an Alliance Separations Module (2695) and a Differential Refractive Index detector (2410). Empower™ software controlled the pump, and recorded and analysed the data. Ammonium acetate (0.05 M, pH 4.75), the eluent, flowed at 0.5 mL min^{-1} through an Ultrahydrogel (UH) 250 column held at 60 °C. The SEC was calibrated for molecular weight using pullulan standards (P800, P400, P200, P100, P50, P20, P10, P5) (Shodex, Japan) injected individually, the Mark–Houwink–Sakurada relation (for the eluent used in this study: $K = 0.00126$ mL g^{-1} and $\alpha = 0.733$ for pullulan, and $K = 0.0544$ mL g^{-1} and $\alpha = 0.486$ for linear starch) (Castro, Ward, et al., 2005), and universal calibration (Grubisic, Rempp, & Benoit, 1967).

The chain-length distributions of phytoglycogen were taken from the literature (Kubo et al., 1999; Nakamura, 2002; Wong et al., 2003) and compared to those of the waxy rice varieties used in this study.

The two size separation methods used here, SEC and FACE, measure different forms of the distribution of debranched chains. FACE measures the number distribution $N(X)$, the number of chains of DP X, while SEC measures what is termed the SEC distribution, $w(\log X)$. The relationship between the two distributions has been discussed extensively elsewhere (Castro, Dumas, et al., 2005; Clay & Gilbert, 1995; Shortt, 1993) and is shown by Eq. (1). This relationship only applies to linear polymers such as debranched chains.

$$w(\log X) = X^2 N(X) \quad (1)$$

2.6. Average sizes from light scattering

Photon correlation spectroscopy (PCS, also termed dynamic light scattering, DLS) provides the z-average of the size of the particles in a dispersion. The use of this technique here is semi-quantitative: to see if there is a significant difference in the z-average sizes of HWI and HWS components (considerable care needs to be exercised with this technique (e.g. Galinsky & Burchard, 1997) for quantitatively reliable results). Here the average size results are tested for artefacts by varying the basic assumptions as to the form of the distribution.

Three varieties were used for the PCS experiment: Hom, Med Gnay and Phae Savan. The separation of HWS and HWI from flour of these varieties was conducted according to modification of a previously published method (Chiou, Fellows, Gilbert, & Fitzgerald, 2005). Prior to dissolution, a protease (Pronase Type XXV from *Streptomyces griseus*, Sigma–Aldrich, St. Louis, MO, USA)–water solution (0.006 U mL^{-1}) was added to the flour (50 mg), and the sample was first incubated at 37 °C to remove storage and surface-bound proteins. The suspension was heated with constant stirring in a closed container (10 min, 95 °C), and then centrifuged (14,000 × g, 10 min). The supernatant contained the HWS fraction, while the pellet contained the HWI fraction.

The water used in the PCS experiments was filtered through a 0.22 μm Millipore filter and then through a 0.02 μm membrane filter (Whatman International Ltd., Maidstone, England). Samples were prepared in duplicate. PCS measurements were conducted at 25 °C with a goniometer (BI-200SM, Brookhaven Instruments, Holtsville, NY, USA) set at a 30° angle and a correlator (BI-200AT, Brookhaven Instruments). A helium–neon laser (632.8 nm, 35 mW, Spectra-Physics, San Jose, CA, USA) served as the light source. Data were collected for 3 min, and deconvoluted using both non-negative least squares (NNLS) and Contin to obtain the diameter of the solubilised molecules in the HWS and the HWI fractions.

2.7. Degree of branching of undebranched fractions

Measurements of the degrees of branching of each fraction of five varieties (Hom, Phae Savan, Laboun, Med Gnay, Mak Fay) were performed as follows. The fractions were freeze-dried, then partially deuterated in D_2O at room temperature for a few hours, after which the suspensions were freeze-dried. The deuteration process was conducted twice. The fractions were then heated at 80 °C with constant shaking (300 rpm, 16 h) in a solution containing anhydrous perdeuterated dimethylsulfoxide (DMSO-d_6) and 0.05 wt% LiBr. D_2O was added to bring the DMSO: D_2O ratio to 3:1 (v/v). The final sample concentrations ranged from 2 to 10 mg mL^{-1} depending on the amount of each fraction. Quantitative ^1H nuclear magnetic resonance (NMR) spectroscopy was conducted on a Bruker Avance 500 spectrometer (Bruker BioSpin, Rheinstetten, Germany) operating at 500.13 MHz at 90 °C with a relaxation delay of 20 s and 64 scans. The signal assignment and calculation of the degree of branching were conducted according to a previously published method (Hernandez et al., 2008). Data were recorded and analysed using the TopSpin® software. Samples were prepared in duplicate.

2.8. Varying conditions affecting the amount of the HWS fraction

It is important to ascertain whether the HWI is truly thermodynamically water-insoluble (meaning that the system is in equilibrium) or a kinetic phenomenon, i.e., the system used does not provide conditions for equilibrium. Two conditions – extraction temperature and extraction time – which would affect the kinetics of solubilisation of the HWS fractions were varied to determine the point at which the amount of HWS components in solution reaches thermodynamic equilibrium: in other words, the point at which the amount of the HWS fraction no longer significantly changes.

2.8.1. Varying extraction temperature

Flour (25 mg) from two waxy varieties (Hom and Med Gnay) was dispersed in water (1.25 mL) for each temperature used in heating: 50, 60, 70, 80, and 95 °C. These mixtures were heated, with stirring, at the different temperatures for 10 min, and then centrifuged. An aliquot of the supernatant (794 μL) was obtained for debranching. The preparation of the flour–water dispersion was performed with five replicates. The starch in each of the collected aliquots was debranched and FACE was conducted for each of the debranched HWS fractions from the different temperatures.

2.8.2. Varying extraction time

The HWS fractions from Hom and Med Gnay were extracted, as described previously, except that heating was conducted at 95 °C for 10, 30, 60, 90 or 120 min. For each heating time, a separate flour–water mixture was prepared. The aliquots from the different heating times were debranched and separated by SEC. Sample preparation and SEC separation were conducted in duplicate. The amount of the HWS fraction was expressed as the total DRI signal from the SEC.

3. Results

3.1. Debranched chain-length distributions

The debranched chain-length distributions of phytoglycogen, obtained from the literature (Kubo et al., 1999; Nakamura, 2002; Wong et al., 2003), were transformed into $\ln N$ plots, and were found to be distinct from those of the HWS fractions of eight waxy rice varieties (Fig. 1). In phytoglycogen, the first maximum occurs at about X 6; in contrast, this maximum was observed at about X 12 for the HWS distributions. Moreover, the $\ln N(X)$ plots of phytoglycogen after this maximum showed an uninterrupted downward slope; however, the $\ln N(X)$ plots of the HWS components showed four regions. The linear downward slope after the first maximum (Region II, X 13–35) was interrupted by an increasing function at about X 35–45 (Region III), and was followed by another linear downward slope (Region IV, $X \geq 45$).

The ratios of sums of $N(X)$ for different ranges of chains (being ratios, these are independent of normalisation) were then compared for the HWS and the HWI fractions of six varieties (Hom, Laboun, Med Gnay, Phae Noy, Mak Fay, and Phae Savan) in the range of chains that can be detected by FACE. These ratios are similar for the two fractions in the six varieties, except for the ratio of X 6–12:X 13–35 in Laboun and in Phae Savan (Table 1).

Fig. 2 gives the SEC distributions $w(\log X)$ of the debranched chains from four waxy varieties, which were then converted to $\ln N(X)$ plots using Eq. (1) (Castro, Dumas, et al., 2005), and are shown in Fig. 3. These $\ln N(X)$ show clearly that higher DP chains

Table 1
Comparison of ratios of $N(X)$ for different chain-length ranges among the flour, the HWS, and the HWI fractions in six waxy rice varieties.

Variety	IRGC Accn Number	Ratio of the sum of $N(X)$ for different chain lengths								
		X 6–12:X 13–35			X 36–45:X 13–35			X 46–62:X 13–35		
		Flour	HWS	HWI	Flour	HWS	HWI	Flour	HWS	HWI
Hom	107140	0.72 ± 0.02[a]	0.68 ± 0.07[a]	0.70 ± 0.01[a]	0.03 ± 0.00[a]	0.05 ± 0.02[a]	0.04 ± 0.02[a]	0.01 ± 0.00[a]	0.03 ± 0.02[a]	0.02 ± 0.01[a]
Med Gnay	107768	0.72 ± 0.01[a]	0.64 ± 0.11[a]	0.73 ± 0.02[a]	0.03 ± 0.00[a]	0.04 ± 0.02[a]	0.03 ± 0.01[a]	0.01 ± 0.00[a]	0.02 ± 0.01[a]	0.01 ± 0.01[a]
Phae Noy	108274	0.69 ± 0.01[a]	0.69 ± 0.02[a]	0.69 ± 0.01[a]	0.05 ± 0.00[a]	0.06 ± 0.01[a]	0.05 ± 0.01[a]	0.04 ± 0.01[a]	0.04 ± 0.01[a]	0.03 ± 0.01[a]
Mak Fay	30112	0.70 ± 0.01[a]	0.69 ± 0.01[a]	0.70 ± 0.01[a]	0.06 ± 0.00[a]	0.06 ± 0.00[a]	0.05 ± 0.00[a]	0.04 ± 0.01[a]	0.05 ± 0.00[a]	0.03 ± 0.01[a]
Laboun	108833	0.72 ± 0.01[b]	0.74 ± 0.01[b]	0.70 ± 0.00[b]	0.03 ± 0.00[a]	0.05 ± 0.02[b]	0.06 ± 0.00[b]	0.01 ± 0.00[a]	0.04 ± 0.01[b]	0.03 ± 0.00[b]
Phae Savan	108287	0.72 ± 0.01[a]	0.74 ± 0.02[b]	0.68 ± 0.00[b]	0.02 ± 0.00[a]	0.06 ± 0.01[b]	0.06 ± 0.00[b]	0.01 ± 0.00[a]	0.04 ± 0.01[b]	0.03 ± 0.00[b]

[a] The means were derived from five replicates.
[b] The means were derived from two replicates.

Fig. 1. Number distributions $N(X)$ obtained by FACE, replotted as $\ln N(X)$ for (A) phytoglycogen from an isoamylase-deficient *sugary-1* mutant (Nakamura, 2002), from EM-914 (Kubo et al., 1999), and from EM-935 (Wong et al., 2003) and (B) HWS fractions from eight representative waxy rice samples (Hom, Med Gnay, Pa Siev 1, Pa Siev 2, Phae Savan, Laboun, Phaehom, Vieng). The $\ln N(X)$ plots are offset for ease of viewing.

are present in the HWI fractions; these chains were not found in the HWS fractions, as indicated by the shorter chain-length distribution in the HWS fractions than the HWI fractions. The HWS fractions all had changes in slope at about X 100, which were not observed in the HWI fractions.

In 56 waxy rice varieties, it was determined that in both HWI and HWS fractions, the short chains ($X \leq 50$) composed 72–73% of the debranched amylopectin distribution while 27–28% of the distribution was composed of chains $X > 50$ (Table 2). The main difference between the two fractions was that the HWI fraction contained chains that were significantly longer than those found in the HWS fraction (Table 2). SEC shows that the longest chain detected from starch in the HWI fractions is approximately 30 DP longer than the longest chains detected in the HWS fraction.

Table 2
Average proportions of short ($X \leq 50$) and long ($X > 50$) chains, and the longest chain detected in debranched amylopectin determined by SEC using UH 250 in 56 waxy rice varieties.

Fraction	% Short chains	% Long chains	Ratio short:long chains	Maximum chain length
HWI	72.0 ± 3.0	28.0 ± 3.0	2.6 ± 0.4	143 ± 15
HWS	72.9 ± 3.6	27.1 ± 3.6	2.7 ± 0.5	117 ± 11

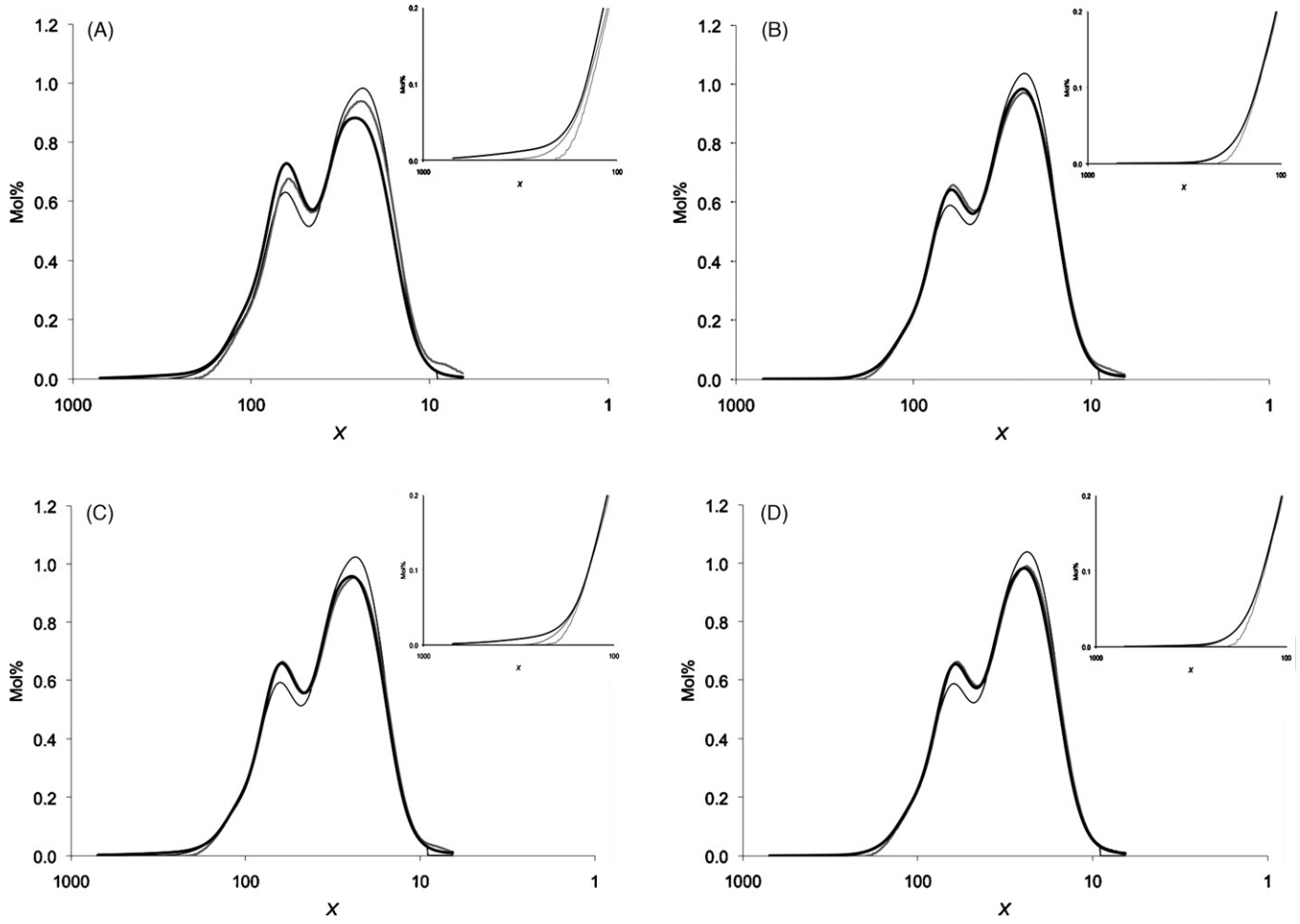

Fig. 2. SEC distributions $w(\log X)$ of debranched flour (thin black line), HWI (thick black line) and HWS (thick grey line) of Hom (A), Med Gnay (B), Laboun (C), and Phae Savan (D) replotted after normalisation. Insets show the differences between the HWS and the HWI at ~X 100.

3.2. Average sizes from light scattering

Table 3 gives the average sizes of Hom, Med Gnay, and Phae Savan HWS and HWI fractions as measured by PCS. This shows that the two algorithms for determining the average diameters, CONTIN and NNLS, of the gelatinised molecules yielded similar averages for all molecules. Both algorithms show that the average size of the gelatinised molecules in the HWS fractions of the three varieties is smaller by about 64–147 nm than the molecules of the HWI fraction.

Table 3
PCS average diameters (nm) of native amylopectin from Hom, Med Gnay, and Phae Savan HWS and HWI fractions. The diameter is the mean of two replicates. The differences between the two methods are not statistically significant.

Variety	Fraction	Diameter (nm)	
		Contin	NNLS
Med Gnay	HWI	383.7	383.3
Hom	HWI	369.0	361.0
Phae Savan	HWI	302.0	307.1
Hom	HWS	296.0	294.9
Phae Savan	HWS	238.2	238.6
Med Gnay	HWS	244.0	236.7

3.3. Degree of branching of undebranched starch in fractions

From the ^{1}H NMR data, the degree of branching per monomer unit in the HWS fraction of the four varieties was found to be higher in the HWS fraction than in the HWI fraction (Table 4).

3.4. Varying conditions affecting the amount of the HWS fraction

The gelatinisation temperatures of the varieties sourced from INGER ranged from 68 to 70 °C (Table 5). The yields of the HWS and the HWI fractions after heating at 95 °C for 10 min were 2.8–3.5 mg and 19.6–20.7 mg, respectively (Table 5).

3.4.1. Varying extraction temperature

One way to determine if equilibrium is attained is to accelerate extraction rates by heating. Fig. 4b shows that the HWS fraction in

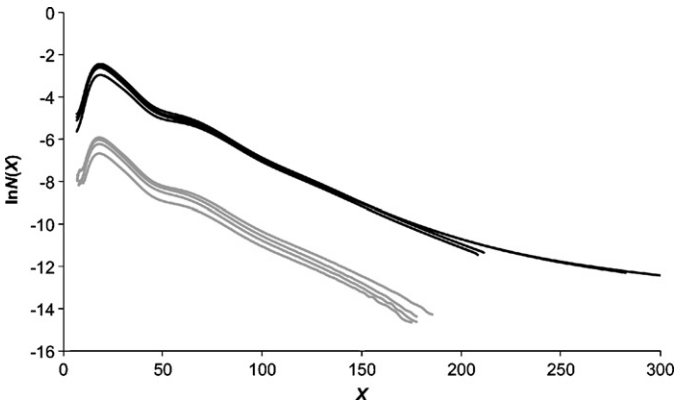

Fig. 3. SEC data of Fig. 2 converted to number distribution $N(X)$ and subsequently plotted as $\ln N(X)$ of debranched HWI (black) and HWS (grey) fractions of the four waxy varieties used in the study.

Table 4
Comparison of the average degrees of branching among the flour, the HWS, and the HWI fractions in four waxy rice varieties (Hom, Med Gnay, Phae Savan, and Laboun). Degree of branching is expressed as the proportion of α-1,6 bonds (%) relative to α-1,4 bonds, and was measured by NMR.

Variety	Fraction	Degree of branching (by NMR, %)[a]
Hom	HWS	4.9[a]
	HWI	4.4 ± 0.0
Laboun	HWS	5.1 ± 0.1
	HWI	4.5 ± 0.1
Med Gnay	HWS	5.0[a]
	HWI	4.4[a]
Phae Savan	HWS	5.0 ± 0.2
	HWI	4.9 ± 0.1

[a] In these fractions, replicates were not available.

Hom did not increase significantly as temperature increased from 50 °C to 80 °C, but at 95 °C the amount of HWS fraction was significantly higher than at 50 °C. By contrast, the amount of material that leached at each temperature from Med Gnay increased as the temperature increased from 50 °C to 70 °C, and after 70 °C, there was no significant increase in the amount that became soluble (Fig. 4a). In both varieties, the HWS fractions obtained at different temperatures had less material than flour.

3.4.2. Varying extraction time

Table 6 shows that there was an increase in the amount of HWS material as the heating time at 95 °C was prolonged. Med Gnay showed almost twice as much HWS material at 10 min than Hom, and after 60 min of heating, there was no difference between the varieties. The amount of HWS material that leached from Med Gnay between 10 and 60 min did not change. However, between 60 and 90 min, there was a large increase in HWS material for both varieties, and no significant change between 90 and 120 min.

Table 5
Gelatinisation temperature of waxy rice varieties used in the study and the amounts of their respective HWS and HWI fractions after heating at 95 °C for 10 min.

Variety	Gelatinisation temperature (°C)	Weight (mg) of each fraction[a]	
		HWS	HWI
Hom	68	3.5 ± 0.2	19.6 ± 0.7
Med Gnay	69	3.4 ± 0.5	19.7 ± 0.3
Phae Noy	67	2.9 ± 0.3	20.6 ± 0.3
Mak Fay	70	3.0 ± 0.6	20.4 ± 0.5
Laboun	67	2.9 ± 0.3	20.1 ± 0.8
Phae Savan	68	2.8 ± 0.2	20.7 ± 0.2

[a] Mean and SD of three replicates.

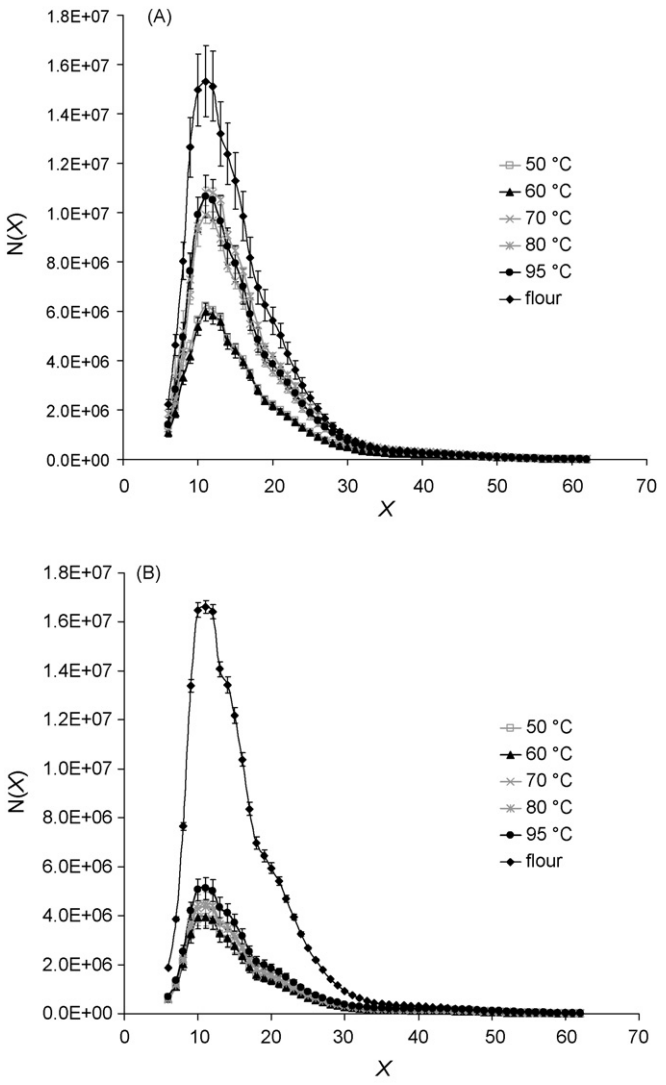

Fig. 4. Chain-length distributions $N(X)$ of flour and of HWS fractions 10 min after extraction at different temperatures (50, 60, 70, 80, 95 °C) from (A) Med Gnay and (B) Hom.

4. Discussion

4.1. Comparing the structure of the HWS fraction and phytoglycogen

Debranched chain-length distributions, plotted as $\ln N(X)$, from rice show four distinct regions (denoted I–IV) for the amylopectin

Table 6
Comparison of the amounts of HWS components, expressed as the total DRI signal of the debranched amylopectin peak separating through the UH 250 in the SEC, leaching out at different heating times in Hom and Med Gnay.

Time (min)	Total DRI signal (mV)	
	Hom	Med Gnay
10	303 ± 1	557 ± 25
30	487 ± 2	563 ± 2
60	596 ± 55	477 ± 49
90	1094 ± 220	1395 ± 30
120	1197 ± 8	1099 ± 20

component, as first seen by Castro, Dumas, et al. (2005). These authors reported that, in contrast to the amylopectin ln $N(X)$ plot, bacterial and mammalian glycogens have only Regions I and II. The non-random Region III is markedly absent in the ln $N(X)$ plots of the samples of glycogen. In the present study, literature data for the chain-length distributions of debranched phytoglycogen from isoamylase-deficient mutants of different botanical origins (Kubo et al., 1999; Nakamura, 2002; Wong et al., 2003) were converted to ln $N(X)$ plots. Fig. 1a shows that the ln $N(X)$ plots of phytoglycogen derived from these mutants had only Regions I and II, similar to the ln $N(X)$ plots of mammalian and bacterial glycogen (Castro, Dumas, et al., 2005). Regions III and IV, found in the HWS plots, Fig. 1b, but absent in the phytoglycogen plots, are typical of amylopectin ln $N(X)$ plots as exhibited by debranched amylopectin from different botanical sources (Castro, Dumas, et al., 2005). The formation of Region III in the ln $N(X)$ plot – the key termination event in the X 35–45 range – is believed to be related to crystallisation (Castro, Dumas, et al., 2005). The presence of Region III in the HWS ln $N(X)$ plots indicates that molecules in the HWS fraction could have some degree of crystallinity; by contrast, the absence of Region III in phytoglycogen ln $N(X)$ plots is consistent with their lack of crystallinity (Nielsen, Baunsgaard, & Blennow, 2002) (it is noted that any extraction of the HWS fraction would destroy any crystallinity these molecules possessed in the native grain). Furthermore, the shape of the ln $N(X)$ plots of the HWS fractions suggests that the HWS fraction is structurally similar to amylopectin, and thus cannot be phytoglycogen. The presence of chains in Region III in the HWS fraction could indicate that there are multiple clusters in its structure, depending on where the chains of Region I and II are attached.

The degrees of branching of the HWS fraction are lower than the levels determined for phytoglycogen, and are comparable to the levels found in amylopectin (Table 4) (Dauvillee et al., 2001; Salomonsson & Sundberg, 1994; Yu et al., 2002). The degrees of branching for maize phytoglycogen are double that of amylopectin (Yun & Matheson, 1993). In *Chlamydomonas* mutants, the degree of branching of phytoglycogen is about 9%, based on ^{1}H NMR measurements (Mouille et al., 1996) and about 13.5% in animal glycogens (Stanek, Falk, & Huber, 1998). The data for degree of branching further strengthen the hypothesis that the material in the HWS fraction is not phytoglycogen.

4.2. Comparing the structure of the HWS fraction with the HWI fraction

For the chain lengths most reliably detected by FACE, those up to about X 35, no significant difference in the ratio of chains between the fractions was found (Table 1); there were also no differences in the proportions of long ($X > 50$) and short chains ($X \leq 50$) between fractions (Table 2). However, SEC is better able to detect longer chains than CE. When the SEC data (Fig. 2) for HWS and HWI fractions were transformed into ln $N(X)$ plots (Fig. 3) – differences in the longer chains are more distinct when plotted this way – the HWS plots showed distinct changes in slope in Region IV at about X 100. This observation is independent of band broadening because the difference in this region is seen in samples analysed under the same conditions. This difference represents an abrupt decrease in the concentration of $X \geq 100$ chains in the HWS fraction. By contrast, the HWI fractions showed a linear negative slope, with a less distinct change in slope at X 100, indicating that the decrease in concentration of long chains in the HWI fractions was more gradual than in the HWS fraction, and led to chain lengths longer than in the HWS fraction. With differences in chain lengths approximately 30 DP between the HWS and the HWI fractions (Table 2), the longer chains are likely to span multiple clusters. The data therefore suggests that clusters in the HWS fraction are borne on shorter chains than clusters in the HWI fraction.

Consistent with the differences in chain length between the fractions, the average size of the hydrated molecules detected by PCS is smaller in the HWS fraction than in the HWI fraction (Table 3). These differences are consistent across several varieties, but it is important to realise the limitations of PCS. First, a solution of (unsegregated) starch molecules has a range of sizes (Rojas, Wahlund, Bergenst, & Nilsson, 2008). Because PCS does not physically separate by size, it cannot give an unambiguous particle size distribution; here only average sizes are examined, not distributions. Next, a starch molecule is not an impenetrable sphere: as well as centre-of-mass diffusion, any part of the chain will also undergo Brownian motion which can introduce artefacts into size measurements (Yang et al., 2006). However, the longer average length of multi-cluster chains in the HWI fraction (Table 2) is consistent with larger molecules in that fraction upon hydration.

Longer multi-cluster chains in the HWI fraction suggest that more clusters are present per long chain than for molecules in the HWS fraction. A difference in chain length of about 30 DP for the long chains suggests that additional clusters could decorate the longer chains in the HWI molecules, depending on the placement of that chain within the molecule. This would explain the lower degree of branching of the molecules in the HWI fraction relative to those in the HWS fraction (Table 4). Tateishi and Nakano (1997) reported that the degree of branching is related to dispersability in aqueous solutions. It is possible that the higher degree of branching makes the HWS fraction more hydrophilic due to an increased presence of hydrogen bonds (Tateishi & Nakano, 1997). The increased solubility could also be associated with decreased intermolecular associations between the branches, thereby decreasing the formation of double helices. By contrast, it is reasonable to suppose that one component of the insolubility of the HWI molecules is caused by co-crystallisation with adjacent molecules at more points, given the greater number of clusters per chain in those molecules; this is akin to entanglement seen in synthetic polymers (Puskas, Chen, Kulbaba, Kaszas, & Soleymannezhad, 2006).

The higher degree of branching of the HWS molecules (Table 4) suggests two possibilities as to the biosynthetic origin of the effect. First, the connectivity of the chains during synthesis of the molecules led to a branching pattern that inhibited the type of crystallisation consistent with amylopectin to occur. One could speculate that this could cause some feedback inhibition of starch synthesis. On the other hand, if synthesis were proceeding efficiently, then the molecules would grow and carry long chains that would subsequently become decorated with clusters, leading to insolubility. Alternatively, the differences in structure could be brought about by differences in the activities of enzymes caused by mutations in the genes coding for these enzymes, which then assumes that the amount of HWS material should be specific to varieties.

4.3. Varying conditions for extracting the HWS fraction: testing for equilibrium

The varieties used in this study, Hom and Med Gnay, had similar gelatinisation temperatures; Hom had 68 °C while Med Gnay had 69 °C (Table 5). The starch granules in these varieties would have started melting and swelling in similar conditions; which implies that dissolution of the HWS components would have begun in similar conditions as well.

The amount of HWS increased with extraction temperature (Fig. 4), which may be attributed to enhanced mobility of molecules, allowing increased penetration of water (Lawal, Adebowale, & Oderlinde, 2004). The increase noted over that range can be explained by the disruption of the starch granules in the processes

following gelatinisation (Atkin, Abeysekera, & Robards, 1998). For Med Gnay, the amount of HWS components was substantially higher at 70 °C compared to that at 50 °C. The amount reached a plateau at 70 °C and no longer increased with increasing temperature (Fig. 4a), For Hom, on the other hand, extraction of the HWS fraction appeared to proceed more slowly than for Med Gnay; however, the increase in amount was significant between 50 °C and 95 °C (Fig. 4b). The slower increase in the amount of the HWS material in Hom suggests that equilibrium had not yet been reached at 95 °C after 10 min of heating. On the other hand, the similar amounts of HWS material in Med Gnay from 70 to 95 °C indicates that there must be a limited amount of HWS material in this variety.

Varying the heating time shows that about twice as much starch leached from Med Gnay than from Hom during the first 10 min of heating (Table 6), indicating that the molecules of Med Gnay are more susceptible to solubilisation than of Hom. This difference is not apparent when determined by weight (Table 5), in which the HWS component also includes non-starch soluble materials, such as proteins. The difference in solubility of the starch components could be due to differences in size between the HWS molecules, and thus the capacity of water to penetrate the granules, and the capacity of the granules to swell. Rather than signify that the amount of the true HWS material is increasing at longer heating periods, the sudden increase in the leached material at 90 min could be caused by degradation of starch molecules with prolonged exposure to heat and shear (Table 6). Thus, there seems to be a limit to the amount of starch that can be dissolved in water; hence, it is presumed that the HWI fraction will not eventually become soluble, indicating that the HWS fraction is a feature of the thermodynamic properties of the different molecules of starch and not just an artefact of the methods used in analyses of starch structure.

5. Summary

This study was conducted to characterise the structural properties of the HWS and the HWI components found in waxy rice. It has been confirmed that the HWS fraction is not phytoglycogen, but has a structure and degree of branching similar to those of amylopectin. There were three main structural differences between the HWS and the HWI fractions: (1) the HWI fraction contained $X \geq 100$ chains, which were absent in the HWS fractions, thus rendering the HWI molecules more likely to be involved in a higher degree of crystallisation with adjacent molecules in the granule and thus be less easily dissolved; (2) the HWS fraction was slightly more branched than the HWI fraction, which increases solubility of the HWS molecules for enthalpic reasons; and (3) the average size of whole starch molecules in the HWS fraction was significantly less than those in the HWI fraction, which decreases the solubility of the HWI because (a) the chains are likely to become more entangled during synthesis and (b) the inference from the Flory–Huggins theory that the free energy of solution of polymers increases with their molecular weight.

Manipulation of extraction conditions (heating temperature and heating time) indicates that the amount of the HWS material must be limited inside the granule, and is not merely an artefact of the extraction method: the amount dissolved was shown to be governed by thermodynamic rather than kinetic considerations. It remains to be determined whether the HWS fraction is specific to varieties and whether the amount or structure impacts upon the sensory properties of rice and other grains.

Acknowledgements

Rosa Paula Cuevas and Melissa Fitzgerald gratefully acknowledge the support of a RIRDC grant (Project no. DAN 212A). The support of an Australian Research Council Discovery grant to RGG (DP0986043) is gratefully acknowledged. The authors thank the TT Chang Genetic Resources Center and the INGER at IRRI for providing the samples used in this study, Dr. Hank de Bruyn for help with the PCS results, and Dr. Marion Gaborieau for conducting NMR experiments.

Appendix A. Supplementary data

Supplementary data associated with this article can be found, in the online version, at doi:10.1016/j.carbpol.2010.03.007.

References

Atkin, N. J., Abeysekera, R. M., & Robards, A. W. (1998). The events leading to the formation of ghost remnants from the starch granule surface and the contribution of the granule surface to the gelatinization endotherm. *Carbohydrate Polymers*, *36*(2–3), 193–204.

Bultosa, G., Hamaker, B. R., & BeMiller, J. N. (2008). An SEC-MALLS study of molecular features of water-soluble amylopectin and amylose of tef [*Eragrostis tef* (Zucc.) Trotter] starches. *Starch Stärke*, *60*(1), 8–22.

Burton, R. A., Jenner, H., Carrangis, L., Fahy, B., Fincher, G. B., Hylton, C., et al. (2002). Starch granule initiation and growth are altered in barley mutants that lack isoamylase activity. *Plant Journal*, *31*(1), 97–112.

Castro, J. V., Dumas, C., Chiou, H., Fitzgerald, M. A., & Gilbert, R. G. (2005). Mechanistic information from analysis of molecular weight distributions of starch. *Biomacromolecules*, *6*(4), 2248–2259.

Castro, J. V., Ward, R. M., Gilbert, R. G., & Fitzgerald, M. A. (2005). Measurement of the molecular weight distribution of debranched starch. *Biomacromolecules*, *6*(4), 2260–2270.

Chinnaswamy, R., & Bhattacharya, K. R. (1986). Characteristics of gel-chromatographic fractions of starch in relation to rice and expanded rice-product qualities. *Starch Stärke*, *38*(2), 51–57.

Chiou, H., Fellows, C. M., Gilbert, R. G., & Fitzgerald, M. A. (2005). Study of rice starch structure by dynamic light scattering in aqueous solution. *Carbohydrate Polymers*, *61*, 61–71.

Clay, P. A., & Gilbert, R. G. (1995). Molecular weight distributions in free-radical polymerizations. 1. Model development and implications for data interpretation. *Macromolecules*, *28*(2), 552–569.

Cowie, J. M. G., & Greenwood, C. T. (1957). Physicochemical studies on starches. Part VI. Aqueous leaching and fractionation of potato starch. *Journal of the Chemical Society*, 2862–2866.

Cuevas, R. P., Daygon, V. D., Corpuz, H. M., Reinke, R. F., Waters, D. L. E., & Fitzgerald, M. A. (2010). Melting the secrets of gelatinisation temperature in rice. *Functional Plant Biology*. in press.

Dauvillee, D., Colleoni, C., Mouille, G., Buleon, A., Gallant, D. J., Bouchet, B., et al. (2001). Two loci control phytoglycogen production in the monocellular green alga *Chlamydomonas reinhardtii*. *Plant Physiology*, *125*, 1710–1722.

Delatte, T., Trevisan, M., Parker, M. L., & Zeeman, S. C. (2005). *Arabidopsis* mutants *Atisa1* and *Atisa2* have identical phenotypes and lack the same multimeric isoamylase, which influences the branch point distribution of amylopectin during starch synthesis. *Plant Journal*, *41*(6), 815–830.

Demorest, D., & Dubrow, R. (1991). Factors influencing the resolution and quantitation of oligonucleotides separated by capillary electrophoresis on a gel-filled capillary. *Journal of Chromatography*, *559*(1–2), 43–56.

Dinges, J. R., Colleoni, C., Myers, A. M., & James, M. G. (2001). Molecular structure of three mutations at the maize *sugary1* locus and their allele-specific phenotypic effects. *Plant Physiology*, *125*, 1406–1418.

Fitzgerald, M. A. (2004). Starch. In E. T. Champagne (Ed.), *Rice chemistry and technology* (pp. 109–142). St. Paul, Minnesota: AACC.

Fujita, N., Kubo, A., Suh, D.-S., Wong, K.-S., Jane, J.-L., Ozawa, K., et al. (2003). Antisense inhibition of isoamylase alters the structure of amylopectin and the physicochemical properties of starch in rice endosperm. *Plant and Cell Physiology*, *44*(6), 607–618.

Galinsky, G., & Burchard, W. (1997). Starch fractions as examples for nonrandomly branched macromolecules. 4. Angular dependence in dynamic light scattering. *Macromolecules*, *30*(22), 6966–6973.

Grubisic, Z., Rempp, P., & Benoit, H. (1967). A universal calibration for gel permeation chromatography. *Journal of Polymer Science Part B: Polymer Physics*, *34*(10), 1707–1713.

Hernandez, J. M., Gaborieau, M., Castignolles, P., Gidley, M. J., Myers, A. M., & Gilbert, R. G. (2008). Mechanistic investigation of a starch-branching enzyme using hydrodynamic volume SEC analysis. *Biomacromolecules*, *9*, 954–965.

Juliano, B. O., Perez, C. M., Kaushik, R. P., & Khush, G. S. (1990). Some grain properties of IR36-based starch mutants. *Starch Stärke*, *42*, 256–260.

Kim, S., & Willett, J. L. (2004). Isolation of amylose from starch solutions by phase separation. *Starch Stärke*, *56*(1), 29–36.

Konkolewicz, D., Taylor, J. W., II, Castignolles, P., Gray-Weale, A., & Gilbert, R. G. (2007). Towards a more general solution to the band-broadening problem in size separation of polymers. *Macromolecules*, *40*(9), 3477–3487.

Kubo, A., Fujita, N., Harada, K., Matsuda, T., Satoh, H., & Nakamura, Y. (1999). The starch-debranching enzymes isoamylase and pullulanase are both involved

in amylopectin biosynthesis in rice endosperm. *Plant Physiology*, *121*(2), 399–409.
Lawal, O. S., Adebowale, K. O., & Oderlinde, R. A. (2004). Functional properties of amylopectin and amylose fractions isolated from bambarra groundnut (*Voandzeia subterranean*) starch. *African Journal of Biotechnology*, *3*(8), 399–404.
Manners, D. J. (1989). Recent developments in our understanding of amylopectin structure. *Carbohydrate Polymers*, *11*, 87–112.
Manners, D. J. (1991). Recent developments in our understanding of glycogen structure. *Carbohydrate Polymers*, *16*(1), 37–82.
Miklus, M. B., & Hamaker, B. R. (2003). Isolation and characterization of a soluble branched starch fraction from corn masa associated with adhesiveness. *Cereal Chemistry*, *80*(6), 693–698.
Mizukami, H., Takeda, Y., & Hizukuri, S. (1999). The structure of the hot-water soluble components in the starch granules of new Japanese rice cultivars. *Carbohydrate Polymers*, *38*(4), 329–335.
Mouille, G., Maddelein, M.-L., Libessart, N., Talaga, P., Decq, A., Delrue, B., et al. (1996). Preamylopectin processing—a mandatory step for starch biosynthesis in plants. *Plant Cell*, *8*(8), 1353–1366.
Myers, A. M., Morell, M. K., James, M. G., & Ball, S. G. (2000). Recent progress toward understanding biosynthesis of the amylopectin crystal. *Plant Physiology*, *122*(4), 989–997.
Nakamura, Y. (2002). Towards a better understanding of the metabolic system for amylopectin biosynthesis in plants: Rice endosperm as a model tissue. *Plant and Cell Physiology*, *43*(7), 718–725.
Nielsen, T. H., Baunsgaard, L., & Blennow, A. (2002). Intermediary glucan structures formed during starch granule biosynthesis are enriched in short side chains, a dynamic pulse labeling approach. *Journal of Biological Chemistry*, *277*(23), 20249–20255.
Ong, M. H., & Blanshard, J. M. V. (1995). Texture determinants of cooked, parboiled rice. II. Physicochemical properties and leaching behavior of rice. *Journal of Cereal Science*, *21*(3), 261–269.
O'Shea, M. G, Samuel, M. S., Konik, C. M., & Morell, M. K. (1998). Fluorophore-assisted carbohydrate electrophoresis (FACE) of oligosaccharides: Efficiency of labelling and high-resolution separation. *Carbohydrate Research*, *307*(1–2), 1–12.
Puskas, J. E., Chen, Y., Kulbaba, K., Kaszas, G., & Soleymannezhad, A. (2006). Effect of the molecular weight and architecture on the size and glass transition of arborescent polyisobutylenes. *Journal of Polymer Science, Part A: Polymer Chemistry*, *44*(5), 1770–1776.
Ramesh, M., Ali, S. Z., & Bhattacharya, K. R. (1999). Starch components in hot-water soluble and insoluble fractions of rice flour. *Starch Stärke*, *51*(8–9), 308–310.
Roger, P., & Colonna, P. (1996). Molecular weight distribution of amylose fractions obtained by aqueous leaching of corn starch. *International Journal of Biological Macromolecules*, *19*(1), 51–61.
Rojas, C. C., Wahlund, K.-G., Bergenst, B., & Nilsson, L. (2008). Macromolecular geometries determined with field-flow fractionation and their impact on the overlap concentration. *Biomacromolecules*, *9*(6), 1684–1690.
Salomonsson, A.-C., & Sundberg, B. (1994). Amylose content and chain profile of amylopectin from normal, high-amylose and waxy barleys. *Starch Stärke*, *46*(9), 325–328.
Shortt, D. W. (1993). Differential molecular weight distributions in high performance size exclusion chromatography. *Journal of Liquid Chromatography & Related Technologies*, *16*(16), 3371–3391.
Slade, L., & Levine, H. (1988). Non-equilibrium melting of native granular starch. Part I. Temperature location of the glass transition associated with gelatinisation of A-type cereal starches. *Carbohydrate Polymers*, *8*, 183–208.
Stanek, M., Falk, H., & Huber, A. (1998). Investigation of the branching characteristic of glycogen by means of two-dimensional ^{1}H and ^{13}C NMR spectroscopy. *Monatshefte für Chemie/Chemical Monthly*, *129*(4), 355–364.
Tateishi, K., & Nakano, A. (1997). Effects of degree of branching on dispersion stability of phytoglycogen in aqueous solution. *Bioscience, Biotechnology, and Biochemistry*, *61*(3), 455–458.
van Berkel, K. Y., Russell, G. T., & Gilbert, R. G. (2005). Molecular weight distributions and chain-stopping events in the free-radical polymerization of methyl methacrylate. *Macromolecules*, *38*(8), 3214–3224.
Ward, R. M., Gao, Q., de Bruyn, H., Gilbert, R. G., & Fitzgerald, M. A. (2006). Improved methods for the structural analysis of the amylose-rich fraction from rice flour. *Biomacromolecules*, *7*(3), 866–876.
Wong, K.-S., Kubo, A., Jane, J.-L., Harada, K., Satoh, H., & Nakamura, Y. (2003). Structures and properties of amylopectin and phytoglycogen in the endosperm of *sugary-1* mutants of rice. *Journal of Cereal Science*, *37*, 139–149.
Yang, C., Meng, B., Chen, M., Liu, X., Hua, Y., & Ni, Z. (2006). Laser-light-scattering study of structure and dynamics of waxy com amylopectin in dilute aqueous solution. *Carbohydrate Polymers*, *64*(2), 190–196.
Yu, S., Blennow, A., Bojko, M., Madsen, F., Olsen, C. E., & Engelsen, S. B. (2002). Physicochemical characterization of floridean starch of red algae. *Starch Stärke*, *54*(2), 66–74.
Yun, S.-H., & Matheson, N. K. (1993). Structures of the amylopectins of waxy, normal, amylose-extender, and wx-ae genotypes and of the phytoglycogen of maize. *Carbohydrate Research*, *243*(2), 307–321.